

# Single-molecule junctions beyond electronic transport

Sriharsha V. Aradhya and Latha Venkataraman\*

**The idea of using individual molecules as active electronic components provided the impetus to develop a variety of experimental platforms to probe their electronic transport properties. Among these, single-molecule junctions in a metal-molecule-metal motif have contributed significantly to our fundamental understanding of the principles required to realize molecular-scale electronic components from resistive wires to reversible switches. The success of these techniques and the growing interest of other disciplines in single-molecule-level characterization are prompting new approaches to investigate metal-molecule-metal junctions with multiple probes. Going beyond electronic transport characterization, these new studies are highlighting both the fundamental and applied aspects of mechanical, optical and thermoelectric properties at the atomic and molecular scales. Furthermore, experimental demonstrations of quantum interference and manipulation of electronic and nuclear spins in single-molecule circuits are heralding new device concepts with no classical analogues. In this Review, we present the emerging methods being used to interrogate multiple properties in single molecule-based devices, detail how these measurements have advanced our understanding of the structure-function relationships in molecular junctions, and discuss the potential for future research and applications.**

Stimulated by the initial proposal that molecules could be used as the functional building blocks in electronic devices<sup>1</sup>, researchers around the world have been probing transport phenomena at the single-molecule level both experimentally and theoretically<sup>2–11</sup>. Recent experimental advances include the demonstration of conductance switching<sup>12–16</sup>, rectification<sup>17–21</sup>, and illustrations on how quantum interference effects<sup>22–26</sup> play a critical role in the electronic properties of single metal–molecule–metal junctions. The focus of these experiments has been to both provide a fundamental understanding of transport phenomena in nanoscale devices as well as to demonstrate the engineering of functionality from rational chemical design in single-molecule junctions. Although so far there are no ‘molecular electronics’ devices manufactured commercially, basic research in this area has advanced significantly. Specifically, the drive to create functional molecular devices has pushed the frontiers of both measurement capabilities and our fundamental understanding of varied physical phenomena at the single-molecule level, including mechanics, thermoelectrics, optoelectronics and spintronics in addition to electronic transport characterizations. Metal–molecule–metal junctions thus represent a powerful template for understanding and controlling these physical and chemical properties at the atomic- and molecular-length scales. In this realm, molecular devices have atomically defined precision that is beyond what is achievable at present with quantum dots. Combined with the vast toolkit afforded by rational molecular design<sup>27</sup>, these techniques hold a significant promise towards the development of actual devices that can transduce a variety of physical stimuli, beyond their proposed utility as electronic elements<sup>28</sup>.

In this Review we discuss recent measurements of physical properties of single metal–molecule–metal junctions that go beyond electronic transport characterizations (Fig. 1). We present insights into experimental investigations of single-molecule junctions under different stimuli: mechanical force, optical illumination and thermal gradients. We then review recent progress in spin- and quantum interference-based phenomena in molecular devices. In what follows, we discuss the emerging experimental

methods, focusing on the scientific significance of investigations enabled by these methods, and their potential for future scientific and technological progress. The details and comparisons of the different experimental platforms used for electronic transport characterization of single-molecule junctions can be found in ref. 29. Together, these varied investigations underscore the importance of single-molecule junctions in current and future research aimed at understanding and controlling a variety of physical interactions at the atomic- and molecular-length scale.

## Structure-function correlations using mechanics

Measurements of electronic properties of nanoscale and molecular junctions do not, in general, provide direct structural information about the junction. Direct imaging with atomic resolution as demonstrated by Ohnishi *et al.*<sup>30</sup> for monoatomic Au wires can be used to correlate structure with electronic properties, however this has not proved feasible for investigating metal–molecule–metal junctions in which carbon-based organic molecules are used. Simultaneous mechanical and electronic measurements provide an alternate method to address questions relating to the structure of atomic-size junctions<sup>31</sup>. Specifically, the measurements of forces across single metal–molecule–metal junctions and of metal point contacts provide independent mechanical information, which can be used to: (1) relate junction structure to conductance, (2) quantify bonding at the molecular scale, and (3) provide a mechanical ‘knob’ that can be used to control transport through nanoscale devices. The first simultaneous measurements of force and conductance in nanoscale junctions were carried out for Au point contacts by Rubio *et al.*<sup>32</sup>, where it was shown that the force data was unambiguously correlated to the quantized changes in conductance. Using a conducting atomic force microscope (AFM) set-up, Tao and coworkers<sup>33</sup> demonstrated simultaneous force and conductance measurements on Au metal–molecule–metal junctions; these experiments were performed at room temperature in a solution of molecules, analogous to the scanning tunnelling microscope (STM)-based break-junction scheme<sup>8</sup> that has now been widely adopted to perform conductance measurements.

Department of Applied Physics and Applied Mathematics, Columbia University, New York, New York 10027, USA.

\*e-mail: lv2117@columbia.edu

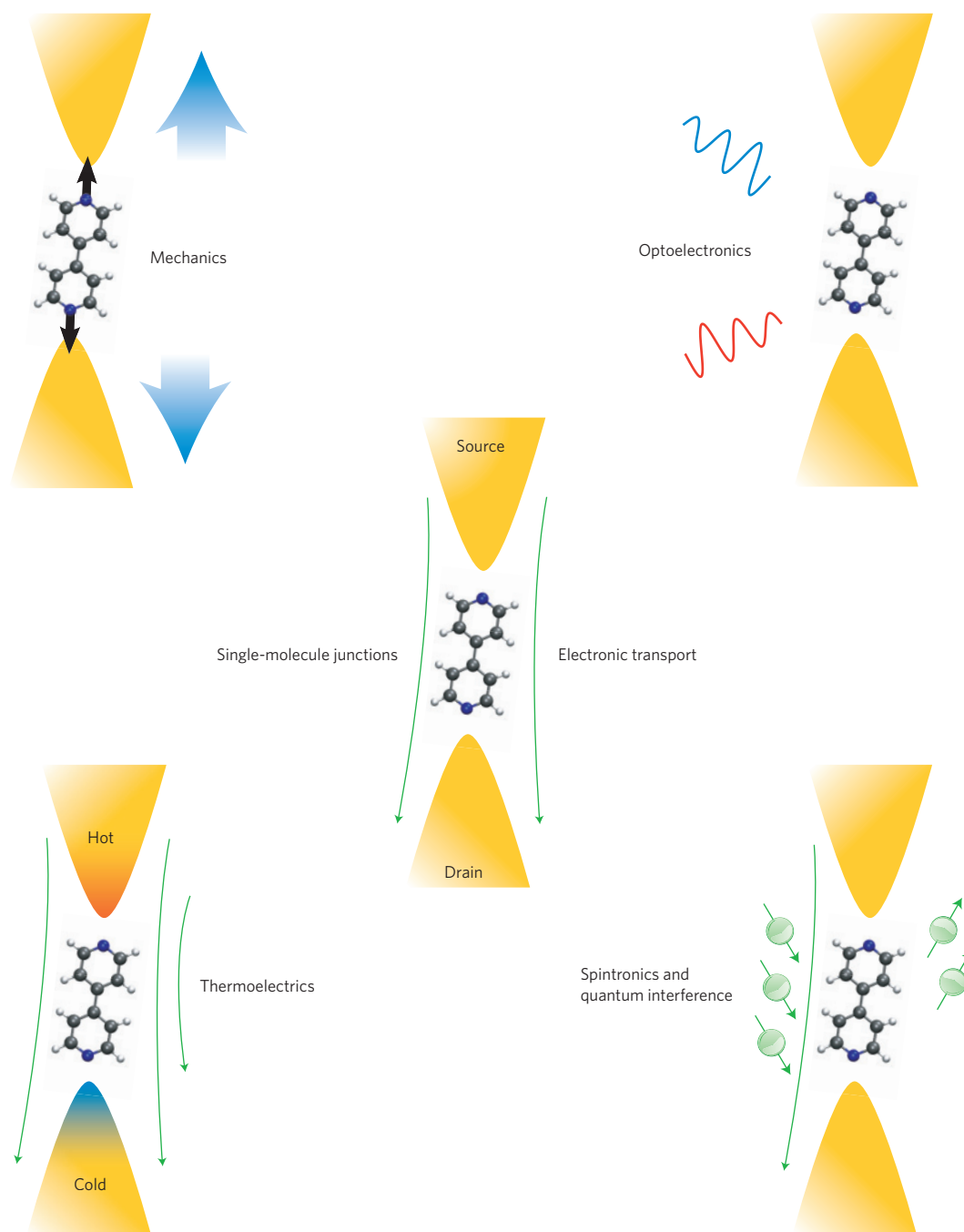


**Figure 1 | Probing multiple properties of single-molecule junctions.** Beyond the electronic transport that led to their initial interest, recent studies are beginning to explore the rich physics of metal-molecule-metal junctions through measurements of mechanics, optical effects and thermoelectric phenomena in addition to demonstrations of quantum mechanical spin- and interference-dependent transport concepts for which there are no analogues in conventional electronics.

These initial experiments relied on the so-called static mode of AFM-based force spectroscopy, where the force on the cantilever is monitored as a function of junction elongation. In this method the deflection of the AFM cantilever is directly related to the force on the junction by Hooke's law (force = cantilever stiffness  $\times$  cantilever deflection). Concurrently, advances in dynamic force spectroscopy — particularly the introduction of the 'q-Plus' configuration<sup>34</sup> that utilizes a very stiff tuning fork as a force sensor — are enabling high-resolution measurements of atomic-size junctions. In this technique, the frequency shift of an AFM cantilever under forced near-resonance oscillation is measured

as a function of junction elongation. This frequency shift can be related to the gradient of the tip-sample force. The underlying advantage of this approach is that frequency-domain measurements of high-Q resonators is significantly easier to carry out with high precision. However, in contrast to the static mode, recovering the junction force from frequency shifts — especially in the presence of dissipation and dynamic structural changes during junction elongation experiments — is non-trivial and a detailed understanding remains to be developed<sup>35</sup>.

The most basic information that can be determined through simultaneous measurement of force and conductance in metal

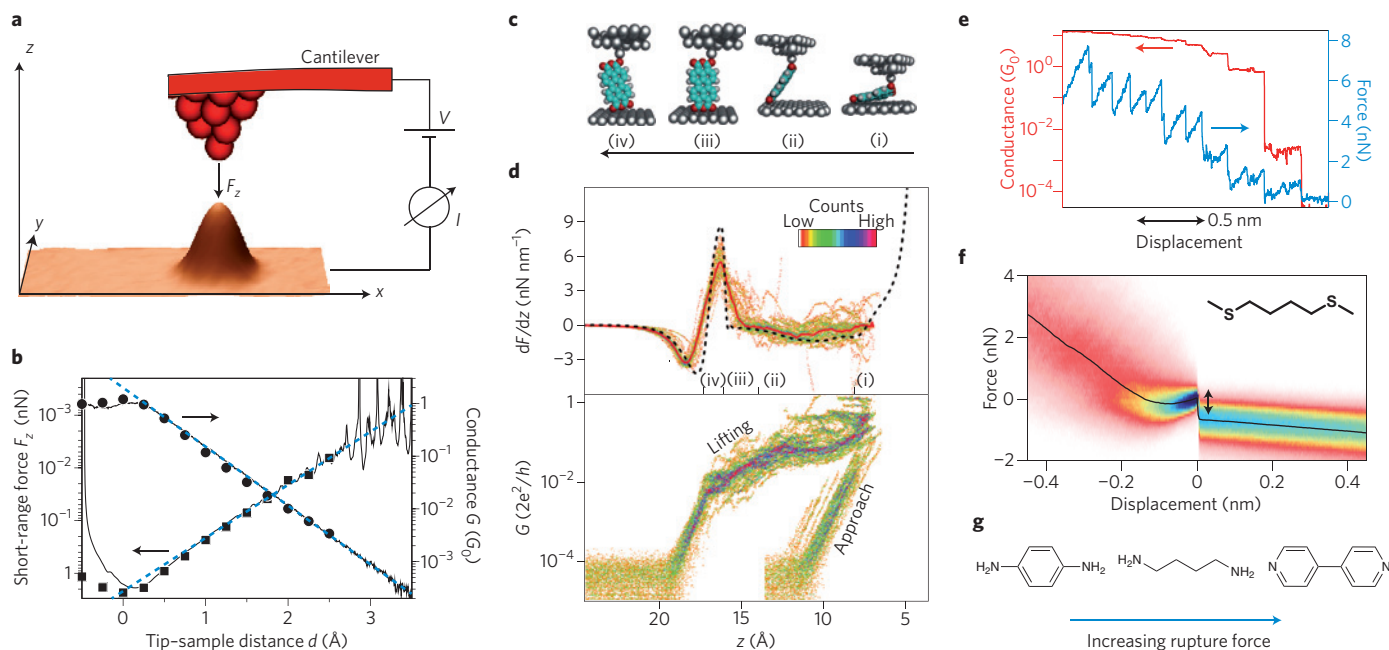


**Figure 2 | Simultaneous measurements of electronic transport and mechanics.** **a**, A conducting AFM set-up with a stiff probe (shown schematically) enabled the atomic-resolution imaging of a Pt adsorbate on a Pt(111) surface (tan colour topography), before the simultaneous measurement of interatomic forces and currents.  $F_z$ , short-range force. **b**, Semilogarithmic plot of tunnelling conductance and  $F_z$  measured over the Pt atom. A similar decay constant for current and force as a function of interatomic distance is seen. The blue dashed lines are exponential fits to the data. **c**, Structural snapshots showing a molecular mechanics simulation of a PTCDA molecule held between a Ag substrate and tip (read right to left). It shows the evolution of the Ag-PTCDA-Ag molecular junction as a function of tip-surface distance. **d**, Upper panel shows experimental stiffness ( $dF/dz$ ) measurements during the lifting process performed with a conducting AFM. The calculated values from the simulation are overlaid (dashed black line). Lower panel shows simultaneously measured conductance ( $G$ ). **e**, Simultaneously measured conductance (red) and force (blue) measurements showing evolution of a molecular junction as a function of junction elongation. A Au point contact is first formed, followed by the formation of a single-molecule junction, which then ruptures on further elongation. **f**, A two-dimensional histogram of thousands of single-molecule junction rupture events (for 1,4-bis(methyl sulphide) butane; inset), constructed by redefining the rupture location as the zero displacement point. The most frequently measured rupture force is the drop in force (shown by the double-headed arrow) at the rupture location in the statistically averaged force trace (overlaid black curve). **g**, Beyond the expected dependence on the terminal group, the rupture force is also sensitive to the molecular backbone, highlighting the interplay between chemical structure and mechanics. In the case of nitrogen-terminated molecules, rupture force increases from aromatic amines to aliphatic amines and the highest rupture force is for molecules with pyridyl moieties. Figure reproduced with permission from: **a,b**, ref. 36, © 2011 APS; **c,d**, ref. 43, © 2011 APS.

contacts is the relation between the measured current and force. An experimental study by Ternes *et al.*<sup>36</sup> attempted to resolve a long-standing theoretical prediction<sup>37</sup> that indicated that both the tunnelling current and force between two atomic-scale metal contacts scale similarly with distance (recently revisited by Jelinek *et al.*<sup>38</sup>). Using the dynamic force microscopy technique, Ternes *et al.* effectively probed the interplay between short-range forces and conductance under ultrahigh-vacuum conditions at liquid helium temperatures. As illustrated in Fig. 2a, the tunnelling current through the gap between the metallic AFM probe and the substrate, and the force on the cantilever were recorded, and both were found to decay exponentially with increasing distance with nearly the same decay constant. Although an exponential decay in current with distance is easily explained by considering an orbital overlap of the tip and sample wavefunctions through a tunnel barrier using Simmons' model<sup>39</sup>, the exponential decay in the short-range forces indicated that perhaps the same orbital controlled the interatomic short-range forces (Fig. 2b).

Using such dynamic force microscopy techniques, researchers have also studied, under ultrahigh-vacuum conditions, forces and conductance across junctions with diatomic adsorbates such as CO (refs 40,41) and more recently with fullerenes<sup>42</sup>, addressing the interplay between electronic transport, binding energetics and structural evolution. In one such experiment, Tautz

and coworkers<sup>43</sup> have demonstrated simultaneous conductance and stiffness measurements during the lifting of a PTCDA (3,4,9,10-perylene-tetracarboxylicacid-dianhydride) molecule from a Ag(111) substrate using the dynamic mode method with an Ag-covered tungsten AFM tip. The authors were able to follow the lifting process (Fig. 2c,d) monitoring the junction stiffness as the molecule was peeled off the surface to yield a vertically bound molecule, which could also be characterized electronically to determine the conductance through the vertical metal-molecule-metal junction with an idealized geometry. These measurements were supported by force field-based model calculations (Fig. 2c and dashed black line in Fig. 2d), presenting a way to correlate local geometry to the electronic transport.

Extending the work from metal point contacts, ambient measurements of force and conductance across single-molecule junctions have been carried out using the static AFM mode<sup>33</sup>. These measurements allow correlation of the bond rupture forces with the chemistry of the linker group and molecular backbone. Single-molecule junctions are formed between a Au-metal substrate and a Au-coated cantilever in an environment of molecules. Measurements of current through the junction under an applied bias determine conductance, while simultaneous measurements of cantilever deflection relate to the force applied across the junction as shown in Fig. 2e. Although measurements of current through

such junctions are easily accomplished using standard instrumentation, measurements of forces with high resolution are not straightforward. This is because a rather stiff cantilever (with a typical spring constant of  $\sim 50 \text{ N m}^{-1}$ ) is typically required to break the Au point contact that is first formed between the tip and substrate, before the molecular junctions are created. The force resolution is then limited by the smallest deflection of the cantilever that can be measured. With a custom-designed system<sup>24</sup> our group has achieved a cantilever displacement resolution of  $\sim 2 \text{ pm}$  (compare with Au atomic diameter of  $\sim 280 \text{ pm}$ ) using an optical detection scheme, allowing the force noise floor of the AFM set-up to be as low as  $0.1 \text{ nN}$  even with these stiff cantilevers (Fig. 2e). With this system, and a novel analysis technique using two-dimensional force–displacement histograms as illustrated in Fig. 2f, we have been able to systematically probe the influence of the chemical linker group<sup>44,45</sup> and the molecular backbone<sup>46</sup> on single-molecule junction rupture force as illustrated in Fig. 2g.

Significant future opportunities with force measurements exist for investigations that go beyond characterizations of the junction rupture force. In two independent reports, one by our group<sup>47</sup> and another by Wagner *et al.*<sup>48</sup>, force measurements were used to quantitatively measure the contribution of van der Waals interactions at the single-molecule level. Wagner *et al.* used the stiffness data from the lifting of PTCDA molecules on a Au(111) surface, and fitted it to the stiffness calculated from model potentials to estimate the contribution of the various interactions between the molecule and the surface<sup>48</sup>. By measuring force and conductance across single 4,4'-bipyridine molecules attached to Au electrodes, we were able to directly quantify the contribution of van der Waals interactions to single-molecule-junction stiffness and rupture force<sup>47</sup>. These experimental measurements can help benchmark the several theoretical frameworks currently under development aiming to reliably capture van der Waals interactions at metal/organic interfaces due to their importance in diverse areas including catalysis, electronic devices and self-assembly.

In most of the experiments mentioned thus far, the measured forces were typically used as a secondary probe of junction properties, instead relying on the junction conductance as the primary signature for the formation of the junction. However, as is the case in large biological molecules<sup>49</sup>, forces measured across single-molecule junctions can also provide the primary signature, thereby making it possible to characterize non-conducting molecules that nonetheless do form junctions. Furthermore, molecules possess many internal degrees of motion (including vibrations and rotations) that can directly influence the electronic transport<sup>50</sup>, and the measurement of forces with such molecules can open up new avenues for mechanochemistry<sup>51</sup>. This potential of using force measurements to elucidate the fundamentals of electronic transport and binding interactions at the single-molecule level is prompting new activity in this area of research<sup>52–54</sup>.

### Optoelectronics and optical spectroscopy

Addressing optical properties and understanding their influence on electronic transport in individual molecular-scale devices, collectively referred to as 'molecular optoelectronics', is an area with potentially important applications<sup>55</sup>. However, the fundamental mismatch between the optical (typically, approximately at the micrometre scale) and molecular-length scales has historically presented a barrier to experimental investigations. The motivations for single-molecule optoelectronic studies are twofold: first, optical spectroscopies (especially Raman spectroscopy) could lead to a significantly better characterization of the local junction structure. The nanostructured metallic electrodes used to realize single-molecule junctions are coincidentally some of the best candidates for local field enhancement due to plasmons (coupled

excitations of surface electrons and incident photons). This therefore provides an excellent opportunity for understanding the interaction of plasmons with molecules at the nanoscale. Second, controlling the electronic transport properties using light as an external stimulus has long been sought as an attractive alternative to a molecular-scale field-effect transistor.

Two independent groups have recently demonstrated simultaneous optical and electrical measurements on molecular junctions with the aim of providing structural information using an optical probe. First, Ward *et al.*<sup>56</sup> used Au nanogaps formed by electromigration<sup>57</sup> to create molecular junctions with a few molecules. They then irradiated these junctions with a laser operating at a wavelength that is close to the plasmon resonance of these Au nanogaps to observe a Raman signal attributable to the molecules<sup>58</sup> (Fig. 3a). As shown in Fig. 3b, they observed correlations between the intensity of the Raman features and magnitude of the junction conductance, providing direct evidence that Raman signatures could be used to identify junction structures. They later extended this experimental approach to estimate vibrational and electronic heating in molecular junctions<sup>59</sup>. For this work, they measured the ratio of the Raman Stokes and anti-Stokes intensities, which were then related to the junction temperature as a function of the applied bias voltage. They found that the anti-Stokes intensity changed with bias voltage while the Stokes intensity remained constant, indicating that the effective temperature of the Raman-active mode was affected by passing current through the junction<sup>60</sup>. Interestingly, Ward *et al.* found that the vibrational mode temperatures exceeded several hundred kelvin, whereas earlier work by Tao and co-workers, who used models for junction rupture derived from biomolecule research, had indicated a much smaller value ( $\sim 10 \text{ K}$ ) for electronic heating<sup>61</sup>. Whether this high temperature determined from the ratio of the anti-Stokes to Stokes intensities indicates that the electronic temperature is also similarly elevated is still being debated<sup>62</sup>, however, one can definitely conclude that such measurements under a high bias (few hundred millivolts) are clearly in a non-equilibrium transport regime, and much more research needs to be performed to understand the details of electronic heating.

Concurrently, Liu *et al.*<sup>62</sup> used the STM-based break-junction technique<sup>8</sup> and combined this with Raman spectroscopy to perform simultaneous conductance and Raman measurements on single-molecule junctions formed between a Au STM tip and a Au(111) substrate. They coupled a laser to a molecular junction as shown in Fig. 3c with a 4,4'-bipyridine molecule bridging the STM tip (top) and the substrate (bottom). Pyridines show clear surface-enhanced Raman signatures on metal<sup>58</sup>, and 4,4'-bipyridine is known to form single-molecule junctions in the STM break-junction set-up<sup>8,15</sup>. Similar to the study of Ward *et al.*<sup>56</sup>, Liu *et al.*<sup>62</sup> found that conducting molecular junctions had a Raman signature that was distinct from the broken molecular junctions. Furthermore, the authors studied the spectra of 4,4'-bipyridine at different bias voltages, ranging from 10 to 800 mV, and reported a reversible splitting of the  $1,609 \text{ cm}^{-1}$  peak (Fig. 3d). Because this Raman signature is due to a ring-stretching mode, they interpreted this splitting as arising from the breaking of the degeneracy between the rings connected to the source and drain electrodes at high biases (Fig. 3c). Innovative experiments such as these have demonstrated that there is new physics to be learned through optical probing of molecular junctions, and are initiating further interest in understanding the effect of local structure and vibrational effects on electronic transport<sup>63</sup>.

Experiments that probe electroluminescence — photon emission induced by a tunnelling current — in these types of molecular junction can also offer insight into structure–conductance correlations. Ho and co-workers have demonstrated simultaneous measurement of differential conductance and photon emission

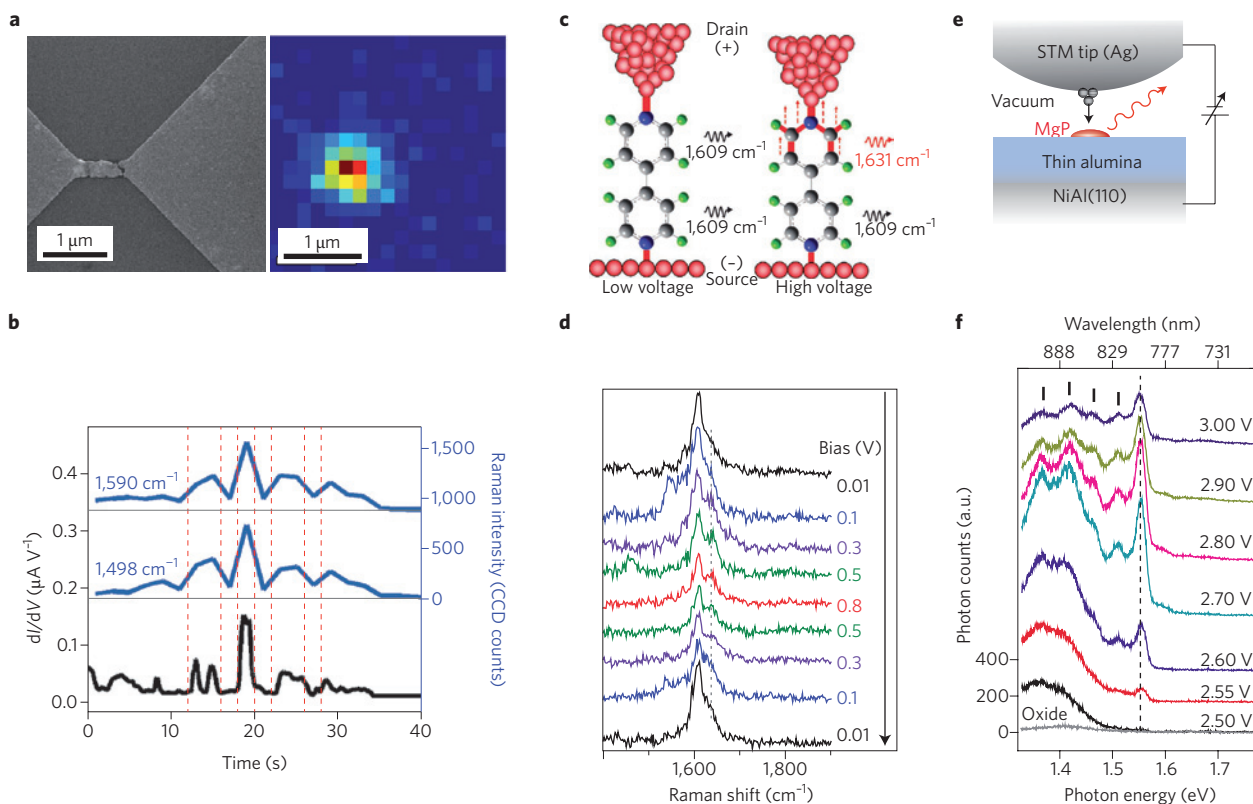


**Figure 3 | Simultaneous studies of optical effects and transport.** **a**, A scanning electron micrograph (left) of an electromigrated Au junction (light contrast) lithographically defined on a Si substrate (darker contrast). The nanoscale gap results in a ‘hot spot’ where Raman signals are enhanced, as seen in the optical image (right). **b**, Simultaneously measured differential conductance (black, bottom) and amplitudes of two molecular Raman features (blue traces, middle and top) as a function of time in a p-mercaptoaniline junction. **c**, Schematic representation of a bipyridine junction formed between a Au STM tip and a Au(111) substrate, where the tip enhancement from the atomically sharp STM tip results in a large enhancement of the Raman signal. **d**, The measured Raman spectra as a function of applied bias indicate breaking of symmetry in the bound molecule. **e**, Schematic representation of a Mg-porphyrin (MgP) molecule sandwiched between a Ag STM tip and a NiAl(110) substrate. A subnanometre alumina insulating layer is a key factor in measuring the molecular electroluminescence, which would otherwise be overshadowed by the metallic substrate. **f**, Emission spectra of a single Mg-porphyrin molecule as a function of bias voltage (data is vertically offset for clarity). At high biases, individual vibronic peaks become apparent. The spectra from a bare oxide layer (grey) is shown for reference. Figure reproduced with permission from: **a,b**, ref. 56, © 2008 ACS; **c,d**, ref. 62, © 2011 NPG; **e,f**, ref. 65, © 2008 APS.

from individual molecules at a submolecular-length scale using an STM<sup>64,65</sup>. Instead of depositing molecules directly on a metal surface, they used an insulating layer to decouple the molecule from the metal<sup>64,65</sup> (Fig. 3e). This critical factor, combined with the vacuum gap with the STM tip, ensures that the metal electrodes do not quench the radiated photons, and therefore the emitted photons carry molecular fingerprints. Indeed, the experimental observation of molecular electroluminescence of C<sub>60</sub> monolayers on Au(110) by Berndt *et al.*<sup>66</sup> was later attributed to plasmon-mediated emission of the metallic electrodes, indirectly modulated by the molecule<sup>67</sup>. The challenge of finding the correct insulator–molecule combination and performing the experiments at low temperature makes electroluminescence relatively uncommon compared with the numerous Raman studies; however, progress is being made on both theoretical and experimental fronts to understand and exploit emission processes in single-molecule junctions<sup>68</sup>.

Beyond measurements of the Raman spectra of molecular junctions, light could be used to control transport in junctions formed with photochromic molecular backbones that occur in two (or more) stable and optically accessible states. Some common examples include azobenzene derivatives, which occur in a *cis* or *trans* form, as well as diarylene compounds that can be switched between a conducting conjugated form and a non-conducting

cross-conjugated form<sup>69</sup>. Experiments probing the conductance changes in molecular devices formed with such compounds have been reviewed in depth elsewhere<sup>70,71</sup>. However, in the single-molecule context, there are relatively few examples of optical modulation of conductance. To a large extent, this is due to the fact that although many molecular systems are known to switch reliably in solution, contact to metallic electrodes can dramatically alter switching properties, presenting a significant challenge to experiments at the single-molecule level.

Two recent experiments have attempted to overcome this challenge and have probed conductance changes in single-molecule junctions while simultaneously illuminating the junctions with visible light<sup>72,73</sup>. Battacharyya *et al.*<sup>72</sup> used a porphyrin-C<sub>60</sub> ‘dyad’ molecule deposited on an indium tin oxide (ITO) substrate to demonstrate the light-induced creation of an excited-state molecule with a different conductance. The unconventional transparent ITO electrode was chosen to provide optical access while also acting as a conducting electrode. The porphyrin segment of the molecule was the chromophore, whereas the C<sub>60</sub> segment served as the electron acceptor. The authors found, surprisingly, that the charge-separated molecule had a much longer lifetime on ITO than in solution. In the break-junction experiments, the illuminated junctions showed a conductance feature that was absent without

light, which the authors assigned to the charge-separated state. In another approach, Lara-Avila *et al.*<sup>73</sup> have reported investigations of a dihydroazulene (DHA)/vinylheptafulvene (VHF) molecule switch, utilizing nanofabricated gaps to perform measurements of Au–DHA–Au single-molecule junctions. Based on the early work by Daub *et al.*<sup>74</sup>, DHA was known to switch to VHF under illumination by 353-nm light and switch back to DHA thermally. In three of four devices, the authors observed a conductance increase after irradiating for a period of 10–20 min. In one of those three devices, they also reported reversible switching after a few hours. Although much more detailed studies are needed to establish the reliability of optical single-molecule switches, these experiments provide new platforms to perform *in situ* investigations of single-molecule conductance under illumination.

We conclude this section by briefly pointing to the rapid progress occurring in the development of optical probes at the single-molecule scale, which is also motivated by the tremendous interest in plasmonics and nano-optics. As mentioned previously, light can be coupled into nanoscale gaps, overcoming experimental challenges such as local heating. Banerjee *et al.*<sup>75</sup> have exploited these concepts to demonstrate plasmon-induced electrical conduction in a network of Au nanoparticles that form metal–molecule–metal junctions between them (Fig. 3f). Although not a single-molecule measurement, the control of molecular conductance through plasmonic coupling can benefit tremendously from the diverse set of new concepts under development in this area, such as nanofabricated transmission lines<sup>76</sup>, adiabatic focusing of surface plasmons, electrical excitation of surface plasmons and nanoparticle optical antennas. The convergence of plasmonics and electronics at the fundamental atomic- and molecular-length scales can be expected to provide significant opportunities for new studies of light–matter interaction<sup>77–79</sup>.

### Thermoelectric characterization of single-molecule junctions

Understanding the electronic response to heating in a single-molecule junction is not only of basic scientific interest; it can have a technological impact by improving our ability to convert wasted heat into usable electricity through the thermoelectric effect, where a temperature difference between two sides of a device induces a voltage drop across it. The efficiency of such a device depends on its thermopower ( $S$ ; also known as the Seebeck coefficient), its electric and thermal conductivity<sup>80</sup>. Strategies for increasing the efficiency of thermoelectric devices turned to nanoscale devices a decade ago<sup>81</sup>, where one could, in principle, increase the electronic conductivity and thermopower while independently minimizing the thermal conductivity<sup>82</sup>. This has motivated the need for a fundamental understanding of thermoelectrics at the single-molecule level<sup>83</sup>, and in particular, the measurement of the Seebeck coefficient in such junctions. The Seebeck coefficient,  $S = -(\Delta V/\Delta T)|_{I=0}$ , determines the magnitude of the voltage developed across the junction when a temperature difference  $\Delta T$  is applied, as illustrated in Fig. 4a; this definition holds both for bulk devices and for single-molecule junctions. If an additional external voltage  $\Delta V$  exists across the junction, then the current  $I$  through the junction is given by  $I = G\Delta V + GS\Delta T$  where  $G$  is the junction conductance<sup>83</sup>. Transport through molecular junctions is typically in the coherent regime where conductance, which is proportional to the electronic transmission probability, is given by the Landauer formula<sup>84</sup>. The Seebeck coefficient at zero applied voltage is then related to the derivative of the transmission probability at the metal Fermi energy (in the off-resonance limit), with,

$$S = - \frac{\pi^2 k_B^2 T}{3e} \left. \frac{\partial \ln(T(E))}{\partial E} \right|_{E_F}$$

where  $k_B$  is the Boltzmann constant,  $e$  is the charge of the electron,

$T(E)$  is the energy-dependent transmission function and  $E_F$  is the Fermi energy. When the transmission function for the junction takes on a simple Lorentzian form<sup>85</sup>, and transport is in the off-resonance limit, the sign of  $S$  can be used to deduce the nature of charge carriers in molecular junctions. In such cases, a positive  $S$  results from hole transport through the highest occupied molecular orbital (HOMO) whereas a negative  $S$  indicates electron transport through the lowest unoccupied molecular orbital (LUMO). Much work has been performed on investigating the low-bias conductance of molecular junctions using a variety of chemical linker groups<sup>86–89</sup>, which, in principle, can change the nature of charge carriers through the junction. Molecular junction thermopower measurements can thus be used to determine the nature of charge carriers, correlating the backbone and linker chemistry with electronic aspects of conduction.

Experimental measurements of  $S$  and conductance were first reported by Ludoph and Ruitenbeek<sup>90</sup> in Au point contacts at liquid helium temperatures. This work provided a method to carry out thermoelectric measurements on molecular junctions. Reddy *et al.*<sup>91</sup> implemented a similar technique in the STM geometry to measure  $S$  of molecular junctions, although due to electronic limitations, they could not simultaneously measure conductance. They used thiol-terminated oligophenyls with 1–3-benzene units and found a positive  $S$  that increased with increasing molecular length (Fig. 4b). These pioneering experiments allowed the identification of hole transport through thiol-terminated molecular junctions, while also introducing a method to quantify  $S$  from statistically significant datasets. Following this work, our group measured the thermoelectric current through a molecular junction held under zero external bias voltage to determine  $S$  and the conductance through the same junction at a finite bias to determine  $G$  (ref. 92). Our measurements showed that amine-terminated molecules conduct through the HOMO whereas pyridine-terminated molecules conduct through the LUMO (Fig. 4b) in good agreement with calculations.

$S$  has now been measured on a variety of molecular junctions demonstrating both hole and electron transport<sup>91–95</sup>. Although the magnitude of  $S$  measured for molecular junctions is small, the fact that it can be tuned by changing the molecule makes these experiments interesting from a scientific perspective. Future work on the measurements of the thermal conductance at the molecular level can be expected to establish a relation between chemical structure and the figure of merit, which defines the thermoelectric efficiencies of such devices and determines their viability for practical applications.

### Spintronics

Whereas most of the explorations of metal–molecule–metal junctions have been motivated by the quest for the ultimate miniaturization of electronic components, the quantum-mechanical aspects that are inherent to single-molecule junctions are inspiring entirely new device concepts with no classical analogues. In this section, we review recent experiments that demonstrate the capability of controlling spin (both electronic and nuclear) in single-molecule devices<sup>96</sup>. The early experiments by the groups of McEuen and Ralph<sup>97</sup>, and Park<sup>98</sup> in 2002 explored spin-dependent transport and the Kondo effect in single-molecule devices, and this topic has recently been reviewed in detail by Scott and Natelson<sup>99</sup>. Here, we focus on new types of experiment that are attempting to control the spin state of a molecule or of the electrons flowing through the molecular junction. These studies are motivated by the appeal of miniaturization and coherent transport afforded by molecular electronics, combined with the great potential of spintronics to create devices for data storage and quantum computation<sup>100</sup>. The experimental platforms for conducting

the spin-dependent transport studies include measurements with (1) non-magnetic electrodes contacting magnetic molecules, (2) magnetic electrodes contacting a non-magnetic molecule, and (3) magnetic electrodes contacting a magnetic molecule.

Experiments with non-magnetic electrodes contacting single magnetic molecules in a transistor configuration have shown a diverse set of phenomena including the demonstration of the Kondo effect<sup>97,98</sup>, the observation of negative differential conductance in electronic transport, as well as the detection and control of magnetic anisotropy<sup>101–103</sup>. In such devices, it was generally not possible to change the spin state of the molecule under investigation. However, in a recent work, van der Zant and co-workers were able to electrically control the spin state of a single-molecule (a Mn-terpyridine derivative) between a ‘high-spin’ ( $S = 5/2$ ) and a ‘low-spin’ ( $S = 1/2$ ) configuration using a gate electrode, as illustrated in Fig. 5a<sup>104</sup>. In crystalline form, the  $5d$  electrons on the Mn core of these molecules are split by their interactions with the ligands, favouring the high-spin state. In this experiment, the authors used the gate electrode to change the charge state of the ligands, enhancing the ligand field strength and therefore stabilizing the low-spin state.

In the second type of experiment, Wulfhchel and co-workers<sup>105</sup> probed the dependence of the conductance of a single non-magnetic molecular junction on the relative alignment of the tip and substrate magnetization. Figure 5b shows the schematic for this STM-based measurement of a phthalocyanine molecule on a Co island on a Cu(111) substrate probed with a Co-coated tungsten tip. Here, the authors found significant differences in the differential conductance of the molecules between the tip and substrate depending on the relative alignment (parallel or antiparallel) of the tip and substrate magnetization. Quantitatively, the conductance with a parallel alignment was found to be ~60% higher on average than the conductance with an antiparallel alignment. Combined with theoretical calculations, these differences were ascribed to spin-dependent hybridization of the molecular orbitals with the electrodes. More recently, a direct experimental observation of the spin-dependent hybridization of  $C_{60}$  molecules on a Cr(001) surface has been obtained using spin-polarized scanning tunnelling microscopy in combination with scanning tunnelling spectroscopy<sup>106</sup>.

Similar spin-polarized STM measurements with magnetic electrodes have also been carried out using magnetic molecules. Generally, in these measurements, differential conductance is measured as a function of tip-sample bias voltage for different relative alignments of the tip and sample magnetization. For example, Bucher and co-workers recently showed that a Co-phthalocyanine molecule on a Co surface can either act as a simple scatterer or as a spin filter, depending on the bias voltage at which the differential conductance is probed<sup>107</sup>. Interestingly, the spin state of a magnetic molecule can change when it interacts with the electrodes; however, this does not necessarily imply that its spin-transport properties are lost. In another experiment with a Co-phthalocyanine molecule, Wiesendanger and co-workers<sup>108</sup> showed that the molecule lost its net spin (and one electron) due to a strong hybridization of the molecular orbitals with the underlying magnetic Fe substrate. Despite this, they still observed a spin-polarized tunnelling current, which they attributed to the molecule–substrate coupling<sup>108</sup>. In a more recent work, Wiesendanger and co-workers were able to spatially visualize spin-split molecular orbitals in a bis(phthalocyaninato) terbium(III) molecule on a Co surface<sup>109</sup>. They again compared the differential conductance while varying the relative orientation of the tip and substrate magnetization, but managed to do so while maintaining subnanometre-scale spatial resolution (Fig. 5c).

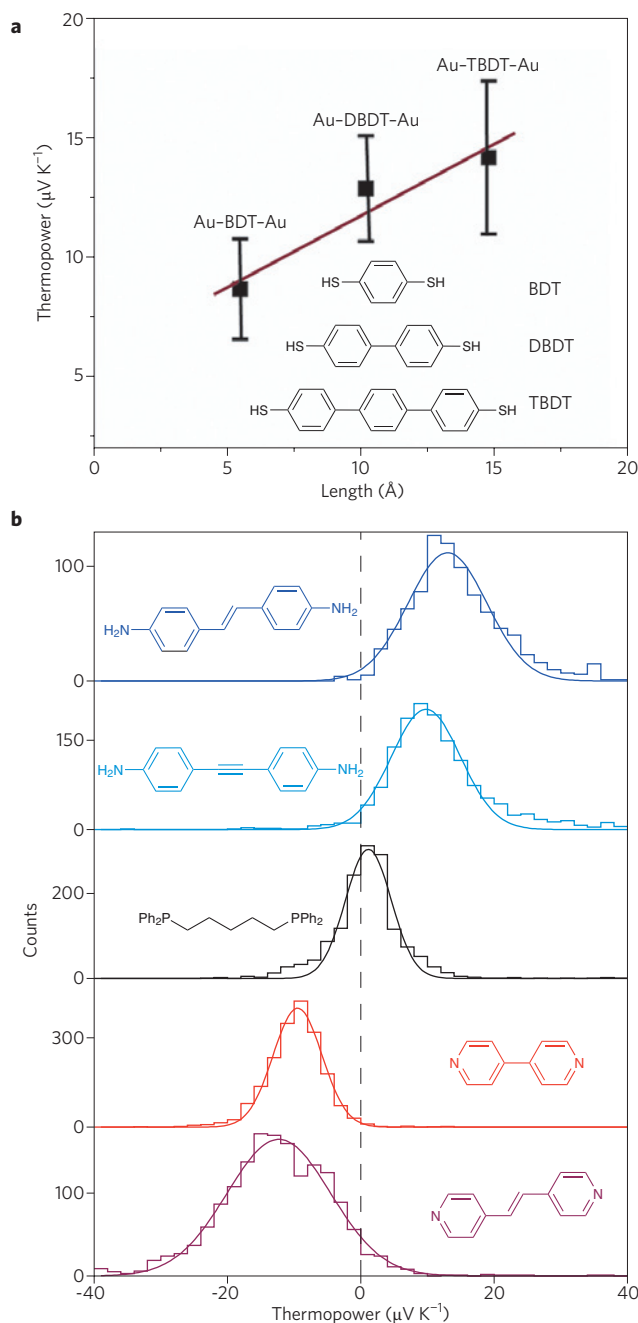


**Figure 4 | Single-molecule thermoelectric characterization.** **a**, Variation of thermopower (Seebeck coefficient) as a function of molecular length in thiol-linked oligophenyl molecules. BDT, 1,4-benzenedithiol; DBDT, 4,4'-dibenzenedithiol; TBDT, 4,4''-tribenzenedithiol. **b**, Statistically relevant measurements of the thermopower reveals hole transport for amines and electron transport for pyridines. Figure reproduced with permission from: **a**, ref. 91, © 2007 AAAS; **b**, ref. 92, © 2012 ACS.

These experiments on molecular and tunnel junctions have advanced our understanding of spin-dependent electron transport. The electronic spins in these molecules are often strongly coupled to the electrodes, and thus controlling them has proved challenging. The stronger the coupling, the shorter the spin-relaxation and coherence times, and therefore devices where the electronic spin state of a molecule can be controlled may prove challenging for applications. Nuclear spins — especially when embedded in a molecule — in contrast, are very weakly coupled to

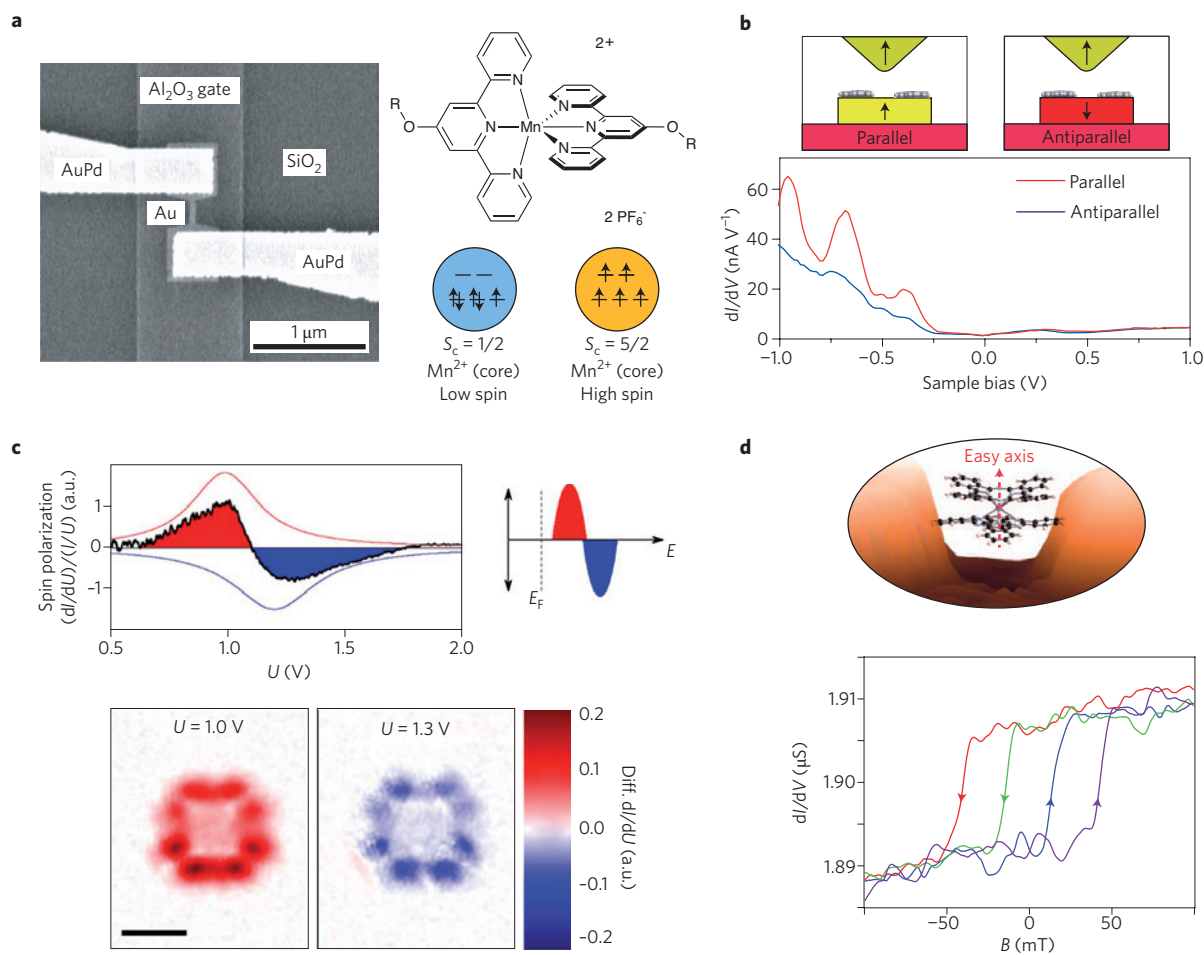


**Figure 5 | Addressing electronic and nuclear spins.** **a**, Scanning electron microscope image of an electromigrated Au junction with an  $\text{Al}_2\text{O}_3$  gate used to study the effect of gating on the spin ground state of a single-molecule magnet (structure and spin states on the right). The voltage on the gate electrode allows for switching between the high- and low-spin states ( $S_c$ ) in the molecule by altering the charge state of the ligands. The structure of the Mn-terpyridine derivative used in this study is shown the upper right panel. **b**, Schematic representation of magnetization orientations (top panels) for phthalocyanine molecules on Co islands probed by a Co-coated tungsten STM tip. The measured differential conductance (bottom) shows clear differences in the transport characteristics depending on the relative alignment of the tip and Co island magnetization. **c**, Experimentally measured spin polarization and schematic representation of spin splitting (top panels) in a single-molecule magnet on a Co surface. The real-space measurements of differential conductance at the energies corresponding to the spin polarizations visualize the identical spatial characteristics of the spin-split orbitals (bottom). Scale bar, 1 nm. **d**, Schematic of a single-molecule magnet in a transistor-configuration set-up, indicating the easy axis of the Tb atom nuclear spin (top). The bottom panel shows multiple differential conductance sweeps (gate voltage =  $-0.9$  V, source-drain voltage =  $0$  V), measured by varying the magnetic field ( $B$ ). The abrupt changes in the conductance of the molecule at characteristic values of the magnetic field (arrows indicate the field-sweep direction) are due to the switching of the Tb magnetic moment. Figure reproduced with permission from: **a**, ref. 104, © 2010 ACS; **b**, ref. 105, © 2011 NPG; **c**, ref. 109, © 2012 NPG; **d**, ref. 110, © 2012 NPG.

the environment, and thus have longer coherence times. However, this weak coupling of the nuclear spin to its environment also makes it extremely challenging to manipulate. In a recent work, Vincent *et al.* demonstrated a new approach to reading the nuclear spin of a terbium atom in a bis(phthalocyaninato)terbium(III) single-molecule device<sup>110</sup>. Figure 5d shows the electronic transport measurements in a transistor configuration that the authors used to not only demonstrate a new technique for reading out the nuclear spin, but also to report its long lifetime (tens of seconds), as determined from analyses of spin relaxation dynamics. Experiments and techniques described here are improving our understanding of magnetic properties at the single-molecule level and are helping to develop practical ways to manipulate spins. These latter aspects could be useful in implementing single-molecule memory, logic and potentially quantum-logic circuit elements.

### Quantum interference

We conclude this Review with a section highlighting another purely quantum mechanical aspect of charge transport through single-molecule junctions — quantum interference — that arises due to the wave nature of the electrons when the device length scale becomes comparable to the electronic phase coherence length. This length-scale criteria is already satisfied by mesoscale devices, as evidenced by experiments demonstrating the Aharonov–Bohm effect in metal rings three decades ago<sup>111</sup>. Experiments at the molecular level are not, however, merely a simple extension of such measurements down to the atomic scale; instead, they provide new insights and methods towards controlling charge transport at the level of the wavefunction through chemical design and, potentially, through electrical control. For example, quantum interference effects can dramatically lower the conductance of a cross-conjugated (or a

*meta*-terminated) molecule when compared with the linearly conjugated (or *para*-terminated) analogue<sup>22,23</sup>. From a chemical perspective, this can be intuitively understood in analogy to the electronic effect of a substituent at *meta*- and *para*- positions on chemical reaction rates, as characterized by the Hammett constants<sup>112</sup>. Formally, the reduced conductance of cross-conjugated molecular junctions is due to an anti-resonance in the junction transmission function<sup>113</sup>. Controlling the position of this anti-resonance, relative to the electrode Fermi level could open up a pathway to create a quantum interference-controlled molecular switch with a potentially large on/off ratio<sup>114–117</sup>. It has also been proposed that one could toggle between a conjugated and cross-conjugated molecular junction through a chemical or conformational change<sup>115,118</sup>. Technologically, the discrete energy levels in a molecular junction can allow for interference effects to be preserved even at high temperatures. Thus the ability to control interference effects encoded in the chemical structure of a molecule will enable novel functionality that can operate at room temperature.

At the most fundamental level, chemical structure controls interference effects in molecular junctions. Thus a molecular structure with two equivalent pathways for conduction should show an increase in conductance when compared with a similar molecule with only a single conduction pathway; this might be imagined as having two resistors in parallel as opposed to a single resistor. Although Kirchoff's law for conventional electronic circuits predicts a doubling of conductance in such cases, constructive interference effects could, in theory, result in an increase of a factor of four or larger<sup>119</sup>. Although conceptually simple, the chemical synthesis of stable molecules with multiple conductive backbones is highly challenging. In a recent experiment, we investigated the conductance superposition law in single-molecule junctions with two parallel paths for conduction to probe constructive interference effects<sup>26</sup>. Figure 6a shows the chemical structures of two of the molecules investigated, consisting of either one or two benzene units bonded together cofacially by a common linker on each end. The conductance measurements showed an enhancement by a factor of ~3, larger than what would be predicted from Kirchoff's law. However, even in this simple case, we did not observe a factor of four increase reported in the constructive interference in metal rings because of subtleties that were evident from calculations of the transmission probabilities through these systems demonstrating that molecular junctions cannot simply be treated as a scaled-down version of mesoscopic devices.

One hurdle in probing transport through single-molecule junctions that show destructive interference effects is that their low-bias conductance is very small. Providing convincing evidence that molecular junctions do form by simply measuring current through these junctions is not sufficient as the through-space component of the current can be larger than the through-'bond' component<sup>120</sup>. Force measurements can provide especially useful information in such cases because they probe junction mechanics independent of conductance. We have recently used this approach to measure conductance and force through two molecules that have linkers at either *meta*- or *para*- positions. These measurements were carried out with two stilbene derivatives<sup>24</sup> terminated with methyl sulphide linkers<sup>86</sup>. Although the *para*-terminated stilbene was known to conduct well, destructive quantum interference effects were expected to yield a low- or non-conducting junction in the *meta*-terminated case. From simultaneous force and conductance measurements, we were able to obtain evidence for junction formation in the force signature despite the lack of conductance in the *meta*-terminated stilbene. This experiment showed that destructive quantum interference is not quenched in single-molecule circuits of these molecules, even at room temperature and in ambient conditions.

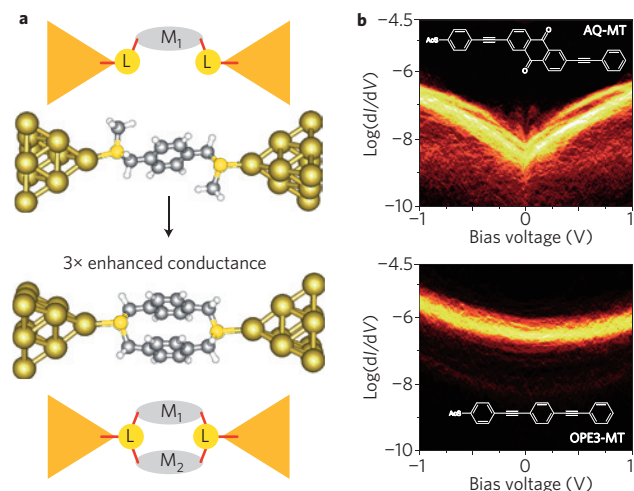


**Figure 6 | Influence of quantum interference on electronic transport.**

**a**, Conceptual sketches (M, molecular backbone; L, chemical linker) and chemical structures of two molecules (S, yellow; Au, gold; C, grey; H, white) used to experimentally probe the role of constructive quantum interference in molecules with parallel conduction pathways. If the molecular circuit was a conventional macroscopic device, a doubling of the conductance for the molecule with two parallel paths would be predicted compared with the molecule with the single pathway. However, the conductance is tripled due to the interplay of constructive quantum interference with the complex transmission characteristics of electronic transport in single-molecule junctions. **b**, Measured conductance ( $dI/dV$ ) versus bias voltage for a cross-conjugated (AQ-MT) and linearly conjugated molecule (OPE3-MT) across hundreds of  $I(V)$  measurements. The sharp dip in the conductance near zero bias results from an anti-resonance in the transmission spectrum and provides evidence for destructive interference in the cross-conjugated molecule. Figure reproduced from: **a**, ref. 26, © 2012 NPG; **b**, ref. 25, © 2012 NPG.

The signature for destructive interference in molecular junctions is the anti-resonance in the transmission probability through the junction; this can, in principle, be probed by measuring the differential conductance of the junction as a function of applied bias voltage. Although this has not been achieved so far in a single-molecule junction where the conductance signal-to-noise ratio can be quite small, Guédon *et al.* were able to show evidence for a transmission anti-resonance in a junction composed of about 100 molecules<sup>25</sup>. They used a conducting AFM technique<sup>121</sup> to measure the differential conductance of molecular junctions in a series of anthraquinone derivatives that were either cross-conjugated or linearly conjugated (Fig. 6b). They observed that the conductance of the cross-conjugated molecular junction was two orders of magnitude lower than that of the linearly conjugated one, even though the difference in their HOMO and LUMO energies was almost the same. Furthermore, the differential conductance measured through the cross-conjugated system showed clear evidence for an anti-resonance, with a sharp dip in the differential conductance close to zero-bias, as shown in Fig. 6b. Although these devices could not be gated electrically in these experiments, the results show that a shift in molecular anti-resonance in such a system by ~0.5 V would yield a two-order-of-magnitude increase in conductance. In contrast, gating the linearly conjugated device by a similar amount would not show a significant change in conductance. These experiments demonstrated the potential for quantum interference-based devices that function at room temperature.

## Summary

From its conception as a path to miniaturize conventional electronic components, to its role in creating new paradigms for quantum mechanically dictated devices, metal–molecule–metal junctions have consistently provided a remarkably fertile platform to study physical phenomena at the molecular scale. Emerging experimental techniques are enabling previously unachievable investigation of a variety of interesting properties, and their correlations, in single-molecule junctions. At the same time, these techniques are continuing to improve our understanding of the structure–function relationships and design principles for the realization of molecular-scale devices. Together, these developments are bringing us closer towards the overarching ambition to build, control, and use functional material and devices from the bottom up.

Received 22 October 2012; accepted 22 April 2013;  
published online 5 June 2013

## References

- Aviram, A. & Ratner, M. A. Molecular rectifiers. *Chem. Phys. Lett.* **29**, 277–283 (1974).  
**This article was the first to propose the use of molecules in electronic devices.**
- Reed, M. A., Zhou, C., Muller, C. J., Burgin, T. P. & Tour, J. M. Conductance of a molecular junction. *Science* **278**, 252–254 (1997).
- Di Ventra, M., Pantelides, S. T. & Lang, N. D. First-principles calculation of transport properties of a molecular device. *Phys. Rev. Lett.* **84**, 979–982 (2000).
- Smit, R. H. M. *et al.* Measurement of the conductance of a hydrogen molecule. *Nature* **419**, 906–909 (2002).  
**This article was the first to demonstrate the use of the break-junction technique to measure currents through a single-molecule junction.**
- Xue, Y. Q., Datta, S. & Ratner, M. A. First-principles based matrix Green's function approach to molecular electronic devices: general formalism. *Chemical Phys.* **281**, 151–170 (2002).
- Reichert, J. *et al.* Driving current through single organic molecules. *Phys. Rev. Lett.* **88**, 176804 (2002).
- Brandbyge, M., Mozos, J. L., Ordejon, P., Taylor, J. & Stokbro, K. Density-functional method for nonequilibrium electron transport. *Phys. Rev. B* **65**, 165401 (2002).
- Xu, B. Q. & Tao, N. J. Measurement of single-molecule resistance by repeated formation of molecular junctions. *Science* **301**, 1221–1223 (2003).  
**This article was the first to implement an STM-based break-junction technique to measure currents through a single-molecule circuit.**
- Selzer, Y. *et al.* Effect of local environment on molecular conduction: Isolated molecule versus self-assembled monolayer. *Nano Lett.* **5**, 61–65 (2005).
- Venkataraman, L., Klare, J. E., Nuckolls, C., Hybertsen, M. S. & Steigerwald, M. L. Dependence of single-molecule junction conductance on molecular conformation. *Nature* **442**, 904–907 (2006).
- Choi, H. J., Marvin, L. C. & Steven, G. L. First-principles scattering-state approach for nonlinear electrical transport in nanostructures. *Phys. Rev. B* **76**, 155420 (2007).
- Chen, F. *et al.* A molecular switch based on potential-induced changes of oxidation state. *Nano Lett.* **5**, 503–506 (2005).
- Lortscher, E., Cizek, J. W., Tour, J. & Riel, H. Reversible and controllable switching of a single-molecule junction. *Small* **2**, 973–977 (2006).
- Liljeroth, P., Repp, J. & Meyer, G. Current-induced hydrogen tautomerization and conductance switching of naphthalocyanine molecules. *Science* **317**, 1203–1206 (2007).
- Quek, S. Y. *et al.* Mechanically controlled binary conductance switching of a single-molecule junction. *Nature Nanotech.* **4**, 230–234 (2009).
- Meisner, J. S. *et al.* A single-molecule potentiometer. *Nano Lett.* **11**, 1575–1579 (2011).
- Metzger, R. M. *et al.* Unimolecular electrical rectification in hexadecylquinolinium tricyanoquinodimethanide. *J. Am. Chem. Soc.* **119**, 10455–10466 (1997).
- Elbing, M. *et al.* A single-molecule diode. *Proc. Natl Acad. Sci. USA* **102**, 8815–8820 (2005).
- Díez-Pérez, I. *et al.* Rectification and stability of a single molecular diode with controlled orientation. *Nature Chem.* **1**, 635–641 (2009).
- Yee, S. K. *et al.* Inverse rectification in donor-acceptor molecular heterojunctions. *ACS Nano* **5**, 9256–9263 (2011).
- Nakamura, H., Asai, Y., Hihath, J., Bruot, C. & Tao, N. Switch of conducting orbital by bias-induced electronic contact asymmetry in a bipyrimidinyl-biphenyl diblock molecule: mechanism to achieve a *pn* directional molecular diode. *The J. Physical Chem. C* **115**, 19931–19938 (2011).
- Mayor, M. *et al.* Electric current through a molecular rod — relevance of the position of the anchor groups. *Angew. Chem. Int. Ed.* **42**, 5834–5838 (2003).
- Taniguchi, M. *et al.* Dependence of single-molecule conductance on molecule junction symmetry. *J. Am. Chem. Soc.* **133**, 11426–11429 (2011).
- Aradhya, S. V. *et al.* Dissecting contact mechanics from quantum interference in single-molecule junctions of stilbene derivatives. *Nano Lett.* **12**, 1643–1647 (2012).
- Guédon, C. M. *et al.* Observation of quantum interference in molecular charge transport. *Nature Nanotech.* **7**, 305–309 (2012).
- Vázquez, H. *et al.* Probing the conductance superposition law in single-molecule circuits with parallel paths. *Nature Nanotech.* **7**, 663–667 (2012).  
**These authors illustrated deviations from Kirchoff's circuit rules using experiments and theoretical calculations of molecular circuits.**
- Bartels, L. Tailoring molecular layers at metal surfaces. *Nature Chem.* **2**, 87–95 (2010).
- Natelson, D. Mechanical break junctions: Enormous information in a nanoscale package. *ACS Nano* **6**, 2871–2876 (2012).
- Akkerman, H. B. & de Boer, B. Electrical conduction through single molecules and self-assembled monolayers. *J. Phys. Condens. Matter* **20**, 013001 (2008).
- Ohnishi, H., Kondo, Y. & Takayanagi, K. Quantized conductance through individual rows of suspended gold atoms. *Nature* **395**, 780–783 (1998).
- Agrait, N., Yeyati, A. L. & van Ruitenbeek, J. M. Quantum properties of atomic-sized conductors. *Phys. Rep.* **377**, 81–279 (2003).
- Rubio, G., Agrait, N. & Vieira, S. Atomic-sized metallic contacts: Mechanical properties and electronic transport. *Phys. Rev. Lett.* **76**, 2302–2305 (1996).
- Xu, B. Q., Xiao, X. Y. & Tao, N. J. Measurements of single-molecule electromechanical properties. *J. Am. Chem. Soc.* **125**, 16164–16165 (2003).  
**This article demonstrated the feasibility of measuring bond rupture forces in molecular junctions using the break-junction method.**
- Giessibl, F. J. Atomic resolution on Si(111)-(7×7) by noncontact atomic force microscopy with a force sensor based on a quartz tuning fork. *Appl. Phys. Lett.* **76**, 1470–1472 (2000).
- Sader, J. E. *et al.* Quantitative force measurements using frequency modulation atomic force microscopy — theoretical foundations. *Nanotechnology* **16**, S94–S101 (2005).
- Ternes, M. *et al.* Interplay of conductance, force, and structural change in metallic point contacts. *Phys. Rev. Lett.* **106**, 016802 (2011).
- Hofer, W. A. & Fisher, A. J. Signature of a chemical bond in the conductance between two metal surfaces. *Phys. Rev. Lett.* **91**, 036803 (2003).
- Jelinek, P., Ondracek, M. & Flores, F. Relation between the chemical force and the tunnelling current in atomic point contacts: a simple model. *J. Phys. Condens. Matter* **24**, 084001 (2012).
- Simmons, J. G. Generalized formula for electric tunnel effect between similar electrodes separated by a thin insulating film. *J. Appl. Phys.* **34**, 1793–1803 (1963).
- Welker, J. & Giessibl, F. J. Revealing the angular symmetry of chemical bonds by atomic force microscopy. *Science* **336**, 444–449 (2012).
- Ternes, M., Lutz, C. P., Hirjibehedin, C. F., Giessibl, F. J. & Heinrich, A. J. The force needed to move an atom on a surface. *Science* **319**, 1066–1069 (2008).
- Nadine, H. *et al.* Force and conductance during contact formation to a C<sub>60</sub> molecule. *New J. Phys.* **14**, 073032 (2012).
- Fournier, N., Wagner, C., Weiss, C., Temirov, R. & Tautz, F. S. Force-controlled lifting of molecular wires. *Phys. Rev. B* **84**, 035435 (2011).
- Frei, M., Aradhya, S. V., Hybertsen, M. S. & Venkataraman, L. Linker dependent bond rupture force measurements in single-molecule junctions. *J. Am. Chem. Soc.* **134**, 4003–4006 (2012).
- Ahn, S. *et al.* Electronic transport and mechanical stability of carboxyl linked single-molecule junctions. *Phys. Chem. Chem. Phys.* **14**, 13841–13845 (2012).
- Frei, M., Aradhya, S. V., Koentopp, M., Hybertsen, M. S. & Venkataraman, L. Mechanics and chemistry: Single molecule bond rupture forces correlate with molecular backbone structure. *Nano Lett.* **11**, 1518–1523 (2011).  
**This article presented the first investigations of the correlations between bond rupture forces with chemical and electronic structure in single-molecule junctions.**
- Aradhya, S. V., Frei, M., Hybertsen, M. S. & Venkataraman, L. Van der Waals interactions at metal/organic interfaces at the single-molecule level. *Nature Mater.* **11**, 872–876 (2012).

48. Wagner, C., Fournier, N., Tautz, F. S. & Temirov, R. Measurement of the binding energies of the organic-metal perylene-teracarboxylic-dianhydride/Au(111) bonds by molecular manipulation using an atomic force microscope. *Phys. Rev. Lett.* **109**, 076102 (2012).
49. Borgia, A., Williams, P. M. & Clarke, J. Single-molecule studies of protein folding. *Annu. Rev. Biochem.* **77**, 101–125 (2008).
50. Ruben, M. *et al.* Charge transport through a carbon-joint molecule. *Small* **4**, 2229–2235 (2008).
51. Franco, I., George, C. B., Solomon, G. C., Schatz, G. C. & Ratner, M. A. Mechanically activated molecular switch through single-molecule pulling. *J. Am. Chem. Soc.* **133**, 2242–2249 (2011).
52. Ilya, V. P. *et al.* An approach to measure electromechanical properties of atomic and molecular junctions. *J. Phys. Condens. Matter* **24**, 164210 (2012).
53. Zhou, J. F., Guo, C. L. & Xu, B. Q. Electron transport properties of single molecular junctions under mechanical modulations. *J. Phys. Condens. Matter* **24**, 164209 (2012).
54. Nef, C., Frederix, P. L. T. M., Brunner, J., Schonenberger, C. & Calame, M. Force-conductance correlation in individual molecular junctions. *Nanotechnology* **23**, 365201 (2012).
55. Galperin, M. & Nitzan, A. Molecular optoelectronics: the interaction of molecular conduction junctions with light. *Phys. Chem. Chem. Phys.* **14**, 9421–9438 (2012).
56. Ward, D. R. *et al.* Simultaneous measurements of electronic conduction and Raman response in molecular junctions. *Nano Lett.* **8**, 919–924 (2008). **This article presents one of the first attempts to simultaneously carry out Raman spectroscopy and charge-transfer measurements through a molecular junction.**
57. Park, H., Lim, A. K. L., Alivisatos, A. P., Park, J. & McEuen, P. L. Fabrication of metallic electrodes with nanometer separation by electromigration. *Appl. Phys. Lett.* **75**, 301–303 (1999).
58. Fleischm, M., Hendra, P. J. & McQuilla, A. Raman-spectra of pyridine adsorbed at a silver electrode. *Chem. Phys. Lett.* **26**, 163–166 (1974).
59. Ward, D. R., Corley, D. A., Tour, J. M. & Natelson, D. Vibrational and electronic heating in nanoscale junctions. *Nature Nanotech.* **6**, 33–38 (2011).
60. Ioffe, Z. *et al.* Detection of heating in current-carrying molecular junctions by Raman scattering. *Nature Nanotech.* **3**, 727–732 (2008).
61. Huang, Z. F., Xu, B. Q., Chen, Y. C., Di Ventra, M. & Tao, N. J. Measurement of current-induced local heating in a single molecule junction. *Nano Lett.* **6**, 1240–1244 (2006).
62. Liu, Z. *et al.* Revealing the molecular structure of single-molecule junctions in different conductance states by fishing-mode tip-enhanced Raman spectroscopy. *Nature Commun.* **2**, 305 (2011).
63. Jiang, N. *et al.* Observation of multiple vibrational modes in ultrahigh vacuum tip-enhanced Raman spectroscopy combined with molecular-resolution scanning tunneling microscopy. *Nano Lett.* **12**, 5061–5067 (2011).
64. Qiu, X. H., Nazin, G. V. & Ho, W. Vibrationally resolved fluorescence excited with submolecular precision. *Science* **299**, 542–546 (2003). **This article presented the first identifiable molecular features in single-molecule photon emission spectra excited by the tunnelling electrons in an STM.**
65. Wu, S. W., Nazin, G. V. & Ho, W. Intramolecular photon emission from a single molecule in a scanning tunneling microscope. *Phys. Rev. B* **77**, 205430 (2008).
66. Berndt, R. *et al.* Photon-emission at molecular resolution induced by a scanning tunneling microscope. *Science* **262**, 1425–1427 (1993).
67. Hoffmann, G., Libioulle, L. & Berndt, R. Tunneling-induced luminescence from adsorbed organic molecules with submolecular lateral resolution. *Phys. Rev. B* **65**, 212107 (2002).
68. Shamai, T. & Selzer, Y. Spectroscopy of molecular junctions. *Chem. Soc. Rev.* **40**, 2293–2305 (2011).
69. Feringa, B. L. *Molecular Switches* (ed. Feringa, B. L.) (Wiley, 2001).
70. Van der Molen, S. J. & Liljeroth, P. Charge transport through molecular switches. *J. Phys. Condens. Matter* **22**, 133001 (2010).
71. Morgenstern, K. Switching individual molecules by light and electrons: From isomerisation to chirality flip. *Prog. Surface Sci.* **86**, 115–161 (2011).
72. Battacharyya, S. *et al.* Optical modulation of molecular conductance. *Nano Lett.* **11**, 2709–2714 (2011).
73. Lara-Avila, S. *et al.* Light-triggered conductance switching in single-molecule dihydroazulene/vinylheptafulvene junctions. *J. Phys. Chem. C* **115**, 18372–18377 (2011).
74. Daub, J., Knochel, T. & Mannschreck, A. Photosensitive dihydroazulenes with chromogenic properties. *Angew. Chem. Int. Ed. Engl.* **23**, 960–961 (1984).
75. Banerjee, P. *et al.* Plasmon-induced electrical conduction in molecular devices. *ACS Nano* **4**, 1019–1025 (2010).
76. Schuller, J. A. *et al.* Plasmonics for extreme light concentration and manipulation. *Nature Mater.* **9**, 193–204 (2010).
77. Ariely, R., Ofarim, A., Noy, G. & Selzer, Y. Accurate determination of plasmonic fields in molecular junctions by current rectification at optical frequencies. *Nano Lett.* **11**, 2968–2972 (2011).
78. Ittah, N. & Selzer, Y. Electrical detection of surface plasmon polaritons by  $1G_0$  gold quantum point contacts. *Nano Lett.* **11**, 529–534 (2011).
79. Savage, K. J. *et al.* Revealing the quantum regime in tunnelling plasmonics. *Nature* **491**, 574–577 (2012).
80. Majumdar, A. Thermoelectricity in semiconductor nanostructures. *Science* **303**, 777–778 (2004).
81. Venkatasubramanian, R., Siivola, E., Colpitts, T. & O'Quinn, B. Thin-film thermoelectric devices with high room-temperature figures of merit. *Nature* **413**, 597–602 (2001).
82. Hochbaum, A. I. *et al.* Enhanced thermoelectric performance of rough silicon nanowires. *Nature* **451**, 163–167 (2008).
83. Dubi, Y. & Di Ventra, M. Heat flow and thermoelectricity in atomic and molecular junctions. *Rev. Mod. Phys.* **83**, 131–155 (2011).
84. Paulsson, M. & Datta, S. Thermoelectric effect in molecular electronics. *Phys. Rev. B* **67**, 241403 (2003).
85. Datta, S. *Electronic Transport in Mesoscopic Systems* (Cambridge Univ. Press, 1995).
86. Park, Y. S. *et al.* Contact chemistry and single-molecule conductance: A comparison of phosphines, methyl sulfides, and amines. *J. Am. Chem. Soc.* **129**, 15768–15769 (2007).
87. Martin, C. A. *et al.* Fullerene-based anchoring groups for molecular electronics. *J. Am. Chem. Soc.* **130**, 13198–13199 (2008).
88. Schneebeli, S. T. *et al.* Single-molecule conductance through multiple  $\pi$ - $\pi$ -stacked benzene rings determined with direct electrode-to-benzene ring connections. *J. Am. Chem. Soc.* **133**, 2136–2139 (2011).
89. Mishchenko, A. *et al.* Single-molecule junctions based on nitrile-terminated biphenyls: A promising new anchoring group. *J. Am. Chem. Soc.* **133**, 184–187 (2011).
90. Ludoph, B. & van Ruitenbeek, J. M. Thermopower of atomic-size metallic contacts. *Phys. Rev. B* **59**, 12290–12293 (1999).
91. Reddy, P., Jang, S. Y., Segalman, R. A. & Majumdar, A. Thermoelectricity in molecular junctions. *Science* **315**, 1568–1571 (2007). **This article described the first measurement of thermopower in molecular junctions.**
92. Widawsky, J. R., Darancet, P., Neaton, J. B. & Venkataraman, L. Simultaneous determination of conductance and thermopower of single molecule junctions. *Nano Lett.* **12**, 354–358 (2012).
93. Malen, J. A. *et al.* Identifying the length dependence of orbital alignment and contact coupling in molecular heterojunctions. *Nano Lett.* **9**, 1164–1169 (2009).
94. Baheti, K. *et al.* Probing the chemistry of molecular heterojunctions using thermoelectricity. *Nano Lett.* **8**, 715–719 (2008).
95. Malen, J. A., Yee, S. K., Majumdar, A. & Segalman, R. A. Fundamentals of energy transport, energy conversion, and thermal properties in organic-inorganic heterojunctions. *Chem. Phys. Lett.* **491**, 109–122 (2010).
96. Sanvito, S. Molecular spintronics. *Chem. Soc. Rev.* **40**, 3336–3355 (2011).
97. Park, J. *et al.* Coulomb blockade and the Kondo effect in single-atom transistors. *Nature* **417**, 722–725 (2002).
98. Liang, W. J., Shores, M. P., Bockrath, M., Long, J. R. & Park, H. Kondo resonance in a single-molecule transistor. *Nature* **417**, 725–729 (2002).
99. Scott, G. D. & Natelson, D. Kondo resonances in molecular devices. *ACS Nano* **4**, 3560–3579 (2010).
100. Bogani, L. & Wernsdorfer, W. Molecular spintronics using single-molecule magnets. *Nature Mater.* **7**, 179–186 (2008).
101. Heersche, H. B. *et al.* Electron transport through single  $Mn_{12}$  molecular magnets. *Phys. Rev. Lett.* **96**, 206801 (2006).
102. Jo, M. H. *et al.* Signatures of molecular magnetism in single-molecule transport spectroscopy. *Nano Lett.* **6**, 2014–2020 (2006).
103. Zyazin, A. S. *et al.* Electric field controlled magnetic anisotropy in a single molecule. *Nano Lett.* **10**, 3307–3311 (2010).
104. Osorio, E. A. *et al.* Electrical manipulation of spin states in a single electrostatically gated transition-metal complex. *Nano Lett.* **10**, 105–110 (2010).
105. Schmaus, S. *et al.* Giant magnetoresistance through a single molecule. *Nature Nanotech.* **6**, 185–189 (2011).
106. Kawahara, S. L. *et al.* Large magnetoresistance through a single molecule due to a spin-split hybridized orbital. *Nano Lett.* **12**, 4558–4563 (2012).
107. Iacovita, C. *et al.* Visualizing the spin of individual cobalt-phthalocyanine molecules. *Phys. Rev. Lett.* **101**, 116602 (2008). **This article presented the first spin-polarized STM measurements showing that a molecule can act as a featureless scatterer or as a spin filter.**

108. Brede, J. *et al.* Spin- and energy-dependent tunneling through a single molecule with intramolecular spatial resolution. *Phys. Rev. Lett.* **105**, 047204 (2010).
109. Schwobel, J. *et al.* Real-space observation of spin-split molecular orbitals of adsorbed single-molecule magnets. *Nature Commun.* **3**, 953 (2012).
110. Vincent, R., Klyatskaya, S., Ruben, M., Wernsdorfer, W. & Balestro, F. Electronic read-out of a single nuclear spin using a molecular spin transistor. *Nature* **488**, 357–360 (2012).  
**This article was the first to demonstrate the use of an electronic signal to read out the nuclear spin state in a single-molecule device.**
111. Webb, R. A., Washburn, S., Umbach, C. P. & Laibowitz, R. B. Observation of  $h/e$  Aharonov–Bohm oscillations in normal-metal rings. *Phys. Rev. Lett.* **54**, 2696–2699 (1985).
112. Hammett, L. P. The effect of structure upon the reactions of organic compounds benzene derivatives. *J. Am. Chem. Soc.* **59**, 96–103 (1937).
113. Sautet, P. & Joachim, C. Electronic interference produced by a benzene embedded in a polyacetylene chain. *Chem. Phys. Lett.* **153**, 511–516 (1988).
114. Baer, R. & Neuhauser, D. Phase coherent electronics: A molecular switch based on quantum interference. *J. Am. Chem. Soc.* **124**, 4200–4201 (2002).
115. Cardamone, D. M., Stafford, C. A. & Mazumdar, S. Controlling quantum transport through a single molecule. *Nano Lett.* **6**, 2422–2426 (2006).
116. Ke, S. H., Yang, W. T. & Baranger, H. U. Quantum-interference-controlled molecular electronics. *Nano Lett.* **8**, 3257–3261 (2008).
117. Markussen, T., Stadler, R. & Thygesen, K. S. The relation between structure and quantum interference in single molecule junctions. *Nano Lett.* **10**, 4260–4265 (2010).
118. Stadler, R., Forshaw, M. & Joachim, C. Modulation of electron transmission for molecular data storage. *Nanotechnology* **14**, 138–142 (2003).
119. Magoga, M. & Joachim, C. Conductance of molecular wires connected or bonded in parallel. *Phys. Rev. B* **59**, 16011 (1999).
120. Solomon, G. C., Herrmann, C., Hansen, T., Mujica, V. & Ratner, M. A. Exploring local currents in molecular junctions. *Nature Chem.* **2**, 223–228 (2010).
121. Cui, X. D. *et al.* Reproducible measurement of single-molecule conductivity. *Science* **294**, 571–574 (2001).

### Acknowledgements

We thank Jonathan Widawsky, Taekyeong Kim and Brian Capozzi for discussions. This work was supported by the National Science Foundation (Career CHE-07-44185) and by the Packard Foundation.

### Additional information

Reprints and permissions information is available online at [www.nature.com/reprints](http://www.nature.com/reprints). Correspondence should be addressed to L.V.

### Competing financial interests

The authors declare no competing financial interests.